JOURNAL OF APPLIED PHYSICS VOLUME 91, NUMBER 5 1 MARCH 2002

Characterization of the bonding strength and interface current of *p*-Si/*n*-InP wafers bonded by surface activated bonding method at room temperature

M. M. R. Howlader,[a] T. Watanabe, and T. Suga
Research Center for Advanced Science and Technology, The University of Tokyo, 4-6-1 Komaba, Meguro-ku, Tokyo 153-8904, Japan

(Received 27 June 2001; accepted for publication 2 November 2001)

Bonding between *p*-Si and *n*-InP was performed through the surface activated bonding method at room temperature. Tensile results show that the samples were visibly separated from the bonded interface, indicating a weak bonding strength. The cause of the weak bonding strength was intensively investigated. Consistent results between x-ray photoelectron spectroscopy and atomic force microscope investigations show that a weak phase of indium is terminated on the InP due to the depletion of phosphorus in the sputtered surface. Existence of indium layers on the debonded Si surface indicate that the samples were separated from the interface of In/InP, but not across the bonded interface of Si and indium. Typical *pn* junction current–voltage behavior indicates no high resistance interface layer that can withstand the flow of current through the interface. Remarkably, sputtering time as well as energy dependence on the interface current is found to be due to the accumulation of sputtering induced defects. © *2002 American Institute of Physics.*
[DOI: 10.1063/1.1430883]

I. INTRODUCTION

Surface activated bonding (SAB) is a solderless unique bonding method that joins two similar and/or dissimilar clean surfaces by means of the adhesive force of surface atoms in an UHV at room temperature RT.[1] Heterogeneous integration between Si and InP through SAB is realized to be indispensable for high efficient optoelectronic devices.[2] The bonding between the lattice mismatched Si and InP through the SAB process can eliminate the high density of dislocations produced in the heteroepitaxial growth process and other conventional bonding techniques, that degrade the crystalline quality. In addition, since the SAB process is performed at RT, the bonded interface does not suffer from thermal stress and threading dislocation. The SAB method has been developed and implemented for the integration of dissimilar materials for quantum devices[3] as well as microelectronic interconnection[2] applications.

Since the SAB method is based on the adhesive force of surface atoms of clean surfaces, the thickness uniformity of the mating surfaces must be high. Moreover, the bonded interface should have enough strength to bear an external mechanical stress and/or polishing load. Electrical measurements, especially $I-V$ characteristics, can give direct information about the condition of the bonded interface unless internal potential barriers withstand carriers. Although the $I-V$ characteristics of an InGaAsP laser fabricated on GaAs[4] substrate by the SAB process at RT were measured, no systematic investigation was done to the interface current of Si and InP bonded by the SAB process. In addition, the precursor for producing active surfaces is the use of a high-energy Ar-fast atom beam (FAB) sputtering source (1.5 keV) that should have a substantial impact on the bonded interface current. Therefore, the effect of sputtering time and energy must be known for the further development of the SAB concept. Consequently, the tensile test as well as $I-V$ measurement of the interface are two measures to assess the bonded interface quality.

The objectives of this work are to bond p-Si/n-InP wafer surfaces using the SAB method at RT, to evaluate the bonding strength and the characteristics of the *pn* junction and, finally, to investigate the time and energy dependent sputtering effect on the interface current.

II. EXPERIMENTAL PROCEDURE

Bare samples of mirror polished (100) *p*-Si and *n*-InP having the sizes of (5×5) and (10×10) mm^2, respectively, were used. The thicknesses of *p*-Si and *n*-InP were 450 and 350 μm, respectively. The resistivity of *p*-Si and *n*-InP was in the ranges of 0.01–0.02 and 0.01–0.03 Ω cm, respectively. Doping elements for *p*-Si and *n*-InP were B and Sn, respectively, with the respective carrier concentration of 5×10^{18} and $1-4\times10^{18}$ cm^{-3}. Generally, the edges of the small sample hinder the bonding between two semiconductors through the SAB method, and, therefore, a surface area of (3×3) mm^2 on the central part of Si to be bonded was masked and the remainder was etched by KOH to a depth of 30 μm. In other words, the mesa structured Si sample was fabricated, thereby the contact area between mating samples was (3×3) mm^2. The *p*-Si sample was cleaned with H_2SO_4 (4) and H_2O_2 (1) solution at 65 °C for 10 min followed by immersion in 3% HF to remove oxide layers. The samples were then boiled in a solution of NH_4OH (1), H_2O_2 (1), and H_2O (5) at 65 °C for 10 min. Samples were rinsed in water

[a]Electronic mail: matiar@su.rcast.u-tokyo.ac.jp

 © 2002 American Institute of Physics

Downloaded 02 Oct 2006 to 130.113.224.243. Redistribution subject to AIP license or copyright, see http://jap.aip.org/jap/copyright.jsp

after each chemical treatment. Finally, the *p*-Si sample was dried by blowing nitrogen on them. The *n*-InP sample was cleaned with acetone and ethanol only.

The samples were separately cleaned by sputtering either with a 0.6 or a 1.5 keV Ar–FAB ion dose rate of 2.38 $\times 10^{14}$ i/cm^2 s in the processing chamber at a pressure of $< 10^{-6}$ Pa for 15–600 s at RT. The etching rate of Si and InP was 0.097 and 0.174 nm/s, respectively, by using a 1.5 keV Ar–FAB with 15 mA. In the case of 0.6 keV with 15 mA, the etching rate is lower. Usually the active surface can be dirty with elapsing time even at an UHV of 10^{-7} Pa, so the samples having active surfaces were transferred to the bonding chamber as quickly as possible, then brought into contact, and, finally, the bonding was performed with a load of 40 kgf at RT. The minimal load is used just for getting the microbended surfaces as close together as possible. Information regarding the SAB apparatus can be seen elsewhere.[5]

III. RESULTS AND DISCUSSION

A. X-ray photoelectron spectroscopy analysis of Si and InP surfaces

Sample surfaces were investigated before and after sputtering using x-ray photoelectron spectroscopy (XPS) from Perkin Elmer with a monochromatic Mg $K\alpha$ x-ray radiation source at 15 kV and 400 kW. Figures 1(a) and 1(b) show the XPS spectra of *p*-Si and *n*-InP, respectively. Both samples were sputtered by using a 1.5 keV Ar–FAB. The sputtering time for *p*-Si was 60 and 180 s, while the sputtering time for *n*-InP was 15 and 30 s. The peaks for *p*-Si before sputtering is less intense because of the termination of native oxide on the surface. Strong peaks for carbon and oxygen are observed on both sample surfaces before sputtering. The peaks of carbon and oxygen before sputtering of both samples disappeared due to the Ar–FAB exposure, indicating the clean and active surfaces were free from native oxide and absorbent. Also, the Ar peak originates from the Ar–FAB source that was implanted into the near surface region of the sample during sputtered cleaning of the sample. As shown in Fig. 1(b), the peaks for phosphorous of *p*-InP is not significant even after sputtering for 30 s. So the depletion of phosphorous is evident even after sputtering for 300 s (not shown). The reason for this depletion is not clearly understood. However, two possible causes can be proposed. One may be that InP decomposes and forms a new compound to InO_2 before sputtering. The other possible cause is that phosphorus may be sputtered away from the surface more so than indium. Therefore, the indium may be terminated abundantly as layers on the InP surface after sputtering. Identical behavior of phosphorus reduction is reported in InP cleaned with a sputtering source of 1.5 keV.[6]

B. Atomic force microscope images of *p*-Si after sputtering and debonding

In order to evaluate the bonding strength of *p*-Si/*n*-InP, tensile tests were performed under atmospheric conditions. All samples were visibly separated from the interface rather than in the bulk region after tensile tests. The average bonding strength was estimated to be 0.03 MPa, which is lower than the bulk strength of bonded materials. Wada and his colleagues have bonded hydrophilic samples of Si and InP at RT and subsequently heated the bonded samples at 700 °C.[7] A bonding strength of 0.3 MPa was measured in their samples, which is ten times higher than that of this work. Although the samples were visibly debonded across the interface in our study, the debonded surfaces needed to be analyzed in order to comprehend the reasons responsible for the low bonding strength.

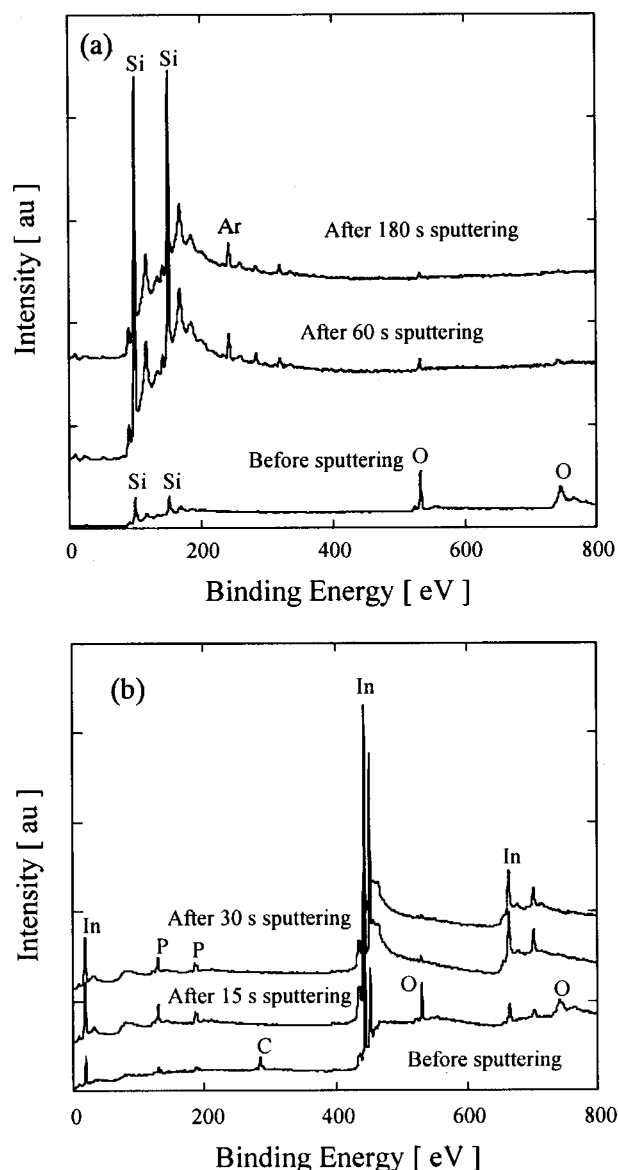

FIG. 1. XPS spectra of (a) *p*-Si and (b) *n*-InP surfaces before and after sputtering with a 0.6 keV Ar–FAB dose rate of 2.38×10^{14} i/cm^2 s for 300 s.

Figure 2 shows the atomic force microscope (AFM) (Seiko Instruments) images of the *p*-Si surface after Ar–FAB sputtering [Fig. 2(a)] and after debonding [Fig. 2(b)]. It can be seen that the surface roughness increases after debonding. The estimated rms values of the surface roughness of *p*-Si after sputtering and after debonding are 0.20 and 7.17 nm, respectively. Reproducible rms values are found in both cases. This fact indicates that a new weak layer of indium may be peeled off from the InP side and transferred to the

Downloaded 02 Oct 2006 to 130.113.224.243. Redistribution subject to AIP license or copyright, see http://jap.aip.org/jap/copyright.jsp

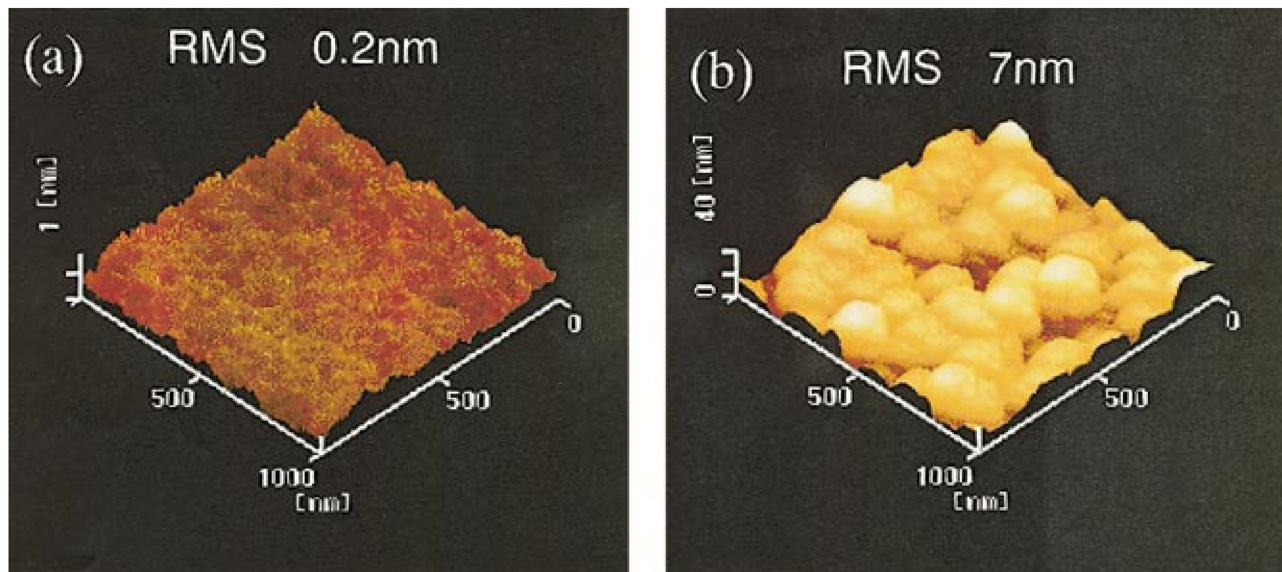

FIG. 2. (Color) AFM images of p-Si (a) before bonding and (b) after debonding.

p-Si surface after debonding, which increases the surface roughness of p-Si.

C. XPS analysis of debonded surfaces

Figure 3 shows the XPS spectra of debonded surfaces of p-Si and n-InP. High intensity peaks of indium on both surfaces are found. In addition, insignificant phosphorous peaks are also visible on the InP surface. The abundance of indium on the InP surface can be seen by comparing Figs. 1(b) and 3. Furthermore, based on the comparison of the Si peak intensity of the debonded Si surface [Fig. 1(b)] to that of the sputtered Si surface, the Si peak intensity of the former is found to be lower than that of the latter due to the termination of indium layers on the p-Si surface. Thus, there is a strong correlation between the AFM and the XPS results. The oxygen and carbon peaks are possibly due to the atmospheric contamination of the debonded surfaces. So the low bonding strength of p-Si and n-InP can be explained in terms of the generation of a new weak phase of indium on n-InP, its peeling from InP, and, finally, its transference to the p-Si surface after debonding.

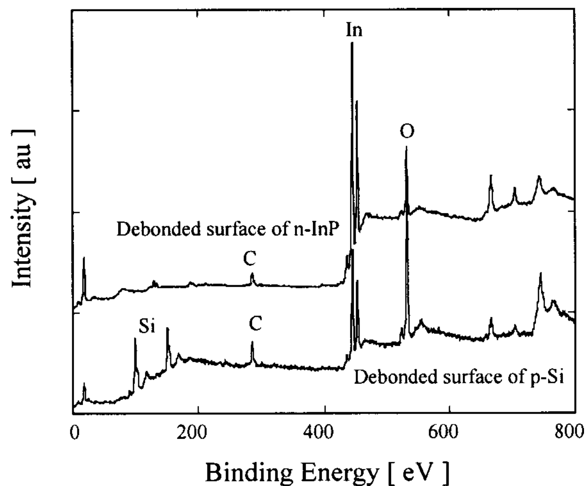

FIG. 3. XPS spectra of p-Si and n-InP after debonding. Debonding was performed under atmospheric conditions and the debonded samples were quickly inserted to the analysis chamber.

D. Theoretical and experimental $I-V$ characteristics

The bonding using the SAB process is performed at RT, so we had to make electrodes for the electrical measurements before the bonding experiment in order to protect the bonded interface from any external heating effect required for ohmic contact. The electrodes were 3 mm in diameter and were made prior to bonding by depositing Au and Ni at RT for p-Si and n-InP, respectively. Then the Ni deposited n-InP sample was annealed at 723 K for 1 min to make an ohmic contact. The heating rate was 150 K/min. Ohmic behavior was achieved in both samples before the bonding experiment. One of the measures of the interface current of a pn junction is to investigate the forward bias current of the bonded interface compared with that of the theoretical results. The $I-V$ characteristics were measured by a Tektronix programable curve tracer (370 A). Ohmic behavior was achieved in both samples before the bonding experiment [Fig. 4(a)]. Generally, the forward biased junction current can be expressed by $I=I_0(e^{qV/nkT}-1)$,[8] where I_0 is the interface current due to carrier generation in the transition region, q is the electron charge, V is the applied potential, k is the Boltzmann's constant, and n is the ideality factor that usually determines the departure from the ideal characteristics. In order to investigate the ideality of the experimental $I-V$ characteristics, the forward bias $I-V$ characteristics of the p-Si/n-InP pn junction were plotted and compared with those of the theoretical behavior at various values of n, and are shown in Fig. 4(b). Experimental results include the data for the interface current of Si/InP samples sputtered with a 1.5 keV Ar–FAB for 30 (Si) and 60 (InP) s and 180 (Si) and 60 (InP) s. Typical pn junction behavior is found for experimental results. One can see that the experimental behavior

Downloaded 02 Oct 2006 to 130.113.224.243. Redistribution subject to AIP license or copyright, see http://jap.aip.org/jap/copyright.jsp

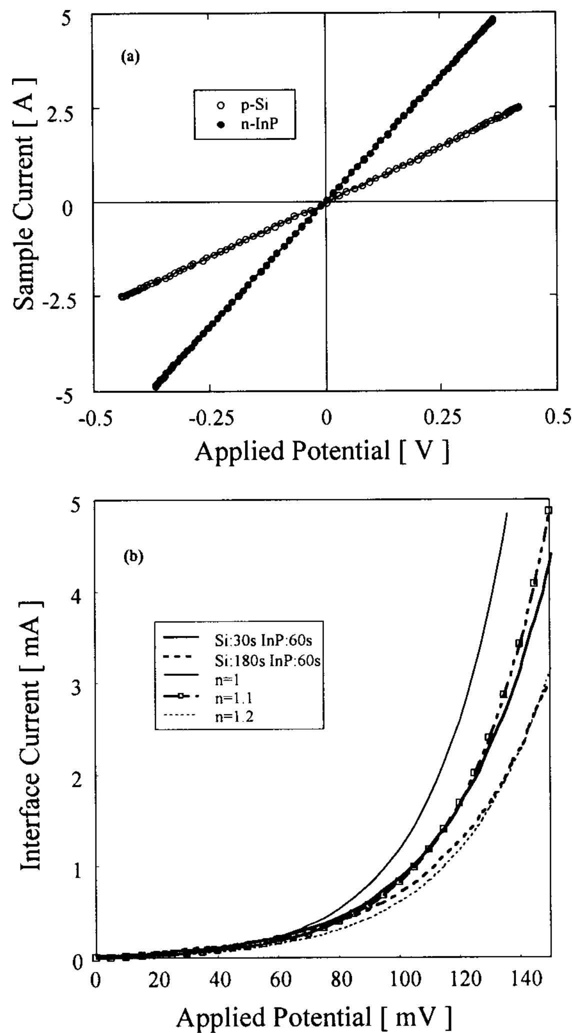

FIG. 4. (a) $I-V$ characteristics of p-Si and n-InP at before the bonding experiment. (b) Comparison of the theoretical and the experimental $I-V$ characteristics of the p-Si/n-InP junction bonded by SAB at RT. Experimental results include the data for the interface current of p-Si/n-InP samples sputtered with a 1.5 keV Ar–FAB for 30 (Si) and 60 (InP) s and 180 (Si) and 60 (InP) s.

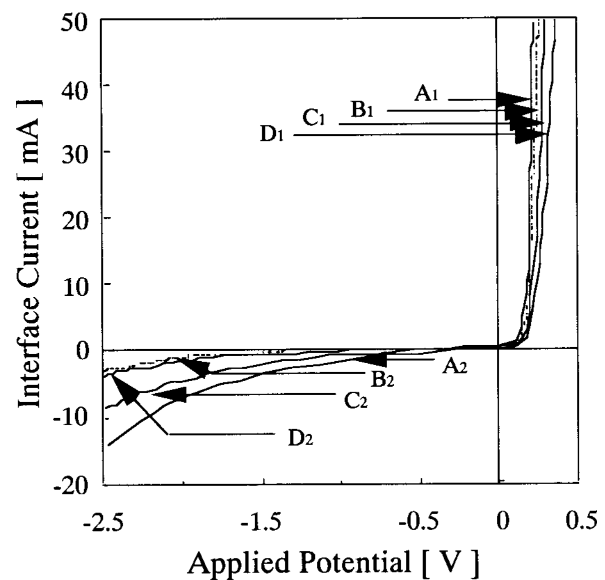

FIG. 5. Ar–FAB time and energy dependence of interface current of p-Si and n-InP bonded by SAB at RT. Subscripts of 1 and 2 represent the curves at forward and reverse bias conditions, respectively. Symbol A represents the curve of p-Si and n-InP interface sputtered for 600 and 60 s, respectively, with a 0.6 keV Ar–FAB. Symbols B, C, and D represent the curves for p-Si and n-InP interfaces sputtered with a 1.5 keV Ar–FAB for 60 (Si) and 30 (InP) s, 300 (Si) and 300 (InP) s, and 600 (Si) and 600 (InP) s. The dose rate in both cases is 2.38×10^{14} i/cm^2 s.

fits to that of the theoretical results within the n values of 1.1 and 1.2. The theoretical calculation is based on the assumption that $I_0=2\times10^{-5}$ A. The fact that the experimental curves fitted closely to those of the theoretical results indicates that the pn junction of Si/InP behaves as an ideal diode.[9] However, we may hypothesize the cause of this ideality. As previously shown, a new weak layer of indium is present between Si and InP. This layer could behave as a Schottky electrode to the Si surface owing to a large work function difference of Si and indium which are 4.85 and 4.0 eV,[10] respectively.

E. Ar–FAB energy and time dependent interface current

The surface cleaning procedure of the SAB method is based on the process of interacting Ar–FAB with the surface atoms which results in sputtering as well as radiation induced damage. Figure 5 shows the sputtering time and energy dependence of the interface currents of the p-Si and the n-InP samples bonded at RT. Typical pn junction behavior is found in all cases and both the forward and reverse bias current is dependent on the sputtering time. In other words, the interface current decreases with increasing sputtering time and vice-versa. An inconsistency is found in the reverse bias current of the samples sputtered for 60 and 30 s, respectively, for n-Si and p-InP. However, the inconsistency is less important than the overall characteristic behavior at reverse bias. All samples exhibit nonsaturated current behavior at reverse bias. Samples A and D have a higher leaky behavior than that of samples B and C. The leaky behavior in the reverse bias current can be explained by the thermal generation of carriers within the transition region.[8,11] Probably the carrier generation in the transition region is a complex function of impurity, lattice defects, and sputtering conditions. In the case of forward bias current, no partial effects like ohmic losses, etc. on the $I-V$ curves are found.

The energy of sputtering source is an important parameter that may control the interface current. As shown in Fig. 5, three measurements are done for samples sputtered with 1.5 keV at various times and only one measurement is done for a sample treated with 0.6 keV. In the case of 1.5 keV energy, the n-Si and p-InP samples are sputtered for 60 (Si) and 30 (InP) s, 300 (Si) and 300 (InP) s, and 600 (Si) and 600 (InP) s. On the other hand, in the case of 0.6 keV energy, p-Si and n-InP are sputtered for 600 and 60 s, respectively. The interface current decreases with increasing sputtering time. Although the sputtering time of the samples treated with 0.6 keV is higher than that of the first set of samples treated with energy 1.5 keV, more current flows in the former both in forward and reverse bias conditions. So a substantial energy dependence of Ar–FAB on the $I-V$ characteristics is

Downloaded 02 Oct 2006 to 130.113.224.243. Redistribution subject to AIP license or copyright, see http://jap.aip.org/jap/copyright.jsp

clearly evident. This behavior can be explained by the damage caused by energetic particles on the semiconductors. Generally, high energy particles cause damage in semiconductors either by displacing atoms from their lattice sites or ionizing atoms. The defects increase with increasing beam energy and irradiation time. Since the penetration depth of energetic particles is proportional to the beam energy, the projected range of 0.6–1.5 keV would be about 200 and 400 nm, respectively.[12] Both displacement and excitation damage can be induced in *p*-Si and *n*-InP. In addition, the sputtering induced point defects can act as precursors for trapping electrons.[13] In fact, an amorphous layer was found to be generated across the interface of Si and InP.[4,14] So the accumulation of sputtering induced defects results in an amorphous layer across the bonded interface and it may control the interface current associated with sample doping. However, these results indicate that the sputtering energy as well as time have a strong influence on the interface current of *p*-Si and *n*-InP.

IV. CONCLUSIONS

Bonding between *p*-Si and *n*-InP has been performed through the SAB method at room temperature. A relatively weak bonding strength is found to be 0.03 MPa. The cause of the weak bonding strength was investigated by XPS and AFM and it was found that a weak phase of indium is terminated on *n*-InP. Additionally, the evidence of existence of indium layers on the debonded Si surface indicate that the samples were separated from the interface of In/InP, but not across the bonded interface of Si and indium. Current–voltage results do not indicate a high resistance interface layer that can withstand the flow of current across the interface. Remarkably, sputtering time as well as energy enhanced behavior on the interface current is found to be due to the accumulation of sputtering induced defects.

ACKNOWLEDGMENTS

The authors would like to thank K. Makoto of Sumitomo Electric Industries, Ltd. for supplying InP samples. Also the assistance of H. Takagi of the Ministry of International Trade and Industry of Japan for the preparation of the Si sample is acknowledged. This work was supported by a Grant-in-Aid for Scientific Research on Priority Areas.

[1] T. Suga, Y. Takahashi, H. Takagi, B. Gibbesch, and G. Elßbner, Acta Metall. Mater. **40**, S133 (1992).
[2] T. R. Chung, N. Hosoda, T. Suga, and H. Takagi, Appl. Phys. Lett. **72**, 1565 (1998).
[3] H. Takagi, K. Kikuchi, R. Maeda, T. R. Chung, and T. Suga, Appl. Phys. Lett. **68**, 2222 (1996).
[4] T. R. Chung, L. Yang, N. Hosoda, H. Takagi, and T. Suga, Appl. Surf. Sci. **117–118**, 808 (1997).
[5] T. Akatsu, G. Sasaki, N. Hosoda, and T. Suga, J. Mater. Res. **12**, 852 (1997).
[6] J. E. Parmeter, R. J. Shul, A. J. Howard, and P. A. Miller, J. Vac. Sci. Technol. B **14**, 3563 (1996).
[7] H. Wada, Y. Ogawa, and T. Kamijoh, Jpn. J. Appl. Phys., **33**, 4878 (1994).
[8] B. G. Streetman, *Solid State Electronic Devices* (Prentice-Hall, Englewood Cliffs, NJ, 1990), p. 178.
[9] N. R. Gardner, N. J. Woods, P. S. Dominguez, E. Z. Tok, C. E. Norman, and J. J. Harris, Semicond. Sci. Technol. **12**, 737 (1997).
[10] S. Halas and T. Durakiewicz, J. Phys.: Condens. Matter **10**, 10815 (1998).
[11] M. M. R. Howlader, T. Watanabe, and T. Suga, J. Vac. Sci. Technol. B **19**, 2114 (2001).
[12] E. L. Hu, C.-H. Chen, and D. L. Green, J. Vac. Sci. Technol. B **14**, 3632 (1996).
[13] S. Murad, M. Rahman, N. Johnson, S. Thoms, S. P. Beaumont, and C. D. W. Wilkinson, J. Vac. Sci. Technol. B **14**, 3658 (1996).
[14] T. R. Chung, L. Yang, N. Hosoda, and T. Suga, Nucl. Instrum. Methods Phys. Res. B **121**, 203 (1997).

Downloaded 02 Oct 2006 to 130.113.224.243. Redistribution subject to AIP license or copyright, see http://jap.aip.org/jap/copyright.jsp